# Systematic study of the lattice dynamics of the uranium rocksalt-structure compounds

J. A. Jackman, T. M. Holden, and W. J. L. Buyers
*Chalk River Nuclear Laboratories, Atomic Energy of Canada Limited, Chalk River, Ontario, Canada K0J 1J0*

P. de V. DuPlessis
*Department of Physics, Rand Afrikaans University, Johannesburg, South Africa*

O. Vogt
*Eidgenössische Technische Hochschule, Zürich, CH-8093 Zürich, Switzerland*

J. Genossar
*Department of Physics, Israel Institute of Technology—Technion, 32000 Haifa, Israel*
(Received 26 August 1985)

The phonon-dispersion relations of USe and UTe have been determined by the inelastic scattering of thermal neutrons. All existing phonon measurements for the U$X$ series, viz., UC, UN, UAs, USb, US, USe, and UTe, have been fitted to the rigid-ion and shell models and dispersion relations have been predicted for UP. The U-$X$ force constants dominate the lattice dynamics and are nearly constant for the series, whereas the U-U force constants vary systematically from being large and positive for the compounds with the smallest lattice parameter to being negative for the chalcogenide series. The negative U-U force constant is identified with destabilizing $f$-$d$ interactions. Elastic constants, derived from the slopes of the dispersion relations and from ultrasound velocity measurements, have been determined. The bulk modulus decreases unusually rapidly as the lattice parameter increases and is in fair agreement with band-structure calculations.

## I. INTRODUCTION

The electronic structure of the uranium compounds, U$X$, which crystallize in the rocksalt structure, has been extensively studied in the last five years. A critical discussion of their properties and unusual behavior may be found in recent reviews.[1,2] Not only do the bulk magnetic properties vary dramatically across the uranium pnictide ($X$=N,P,As,Sb,Bi) and uranium chalcogenide ($X$=S,Se,Te) series, but there is evidence that the nature of the magnetism changes from localized to itinerant as the distance between uranium atoms decreases.[3] While magnetic properties constitute one window on the electronic structure of the valence and conduction electrons, these same electrons govern the interatomic forces which, in turn, determine the phonon frequencies.

A systematic study of the phonons in all U$X$ compounds measured up to the present time is reported in this paper. The study includes previously unpublished dispersion relations for USe and UTe as well as those published elsewhere, viz., for UC (Refs. 4 and 5) (measured at the Oak Ridge National Laboratory), UAs and USb (Ref. 6) (Institut-Laue-Langevin, Grenoble), UN (Ref. 7) and US (Ref. 8) (Chalk River Nuclear Laboratories).

From simple valence considerations, one expects the configuration of the uranium ion to be $5f^2$ for UC, $5f^3$ or $5f^26d^1$ for the pnictides, and $5f^36d^1$ for the chalcogenides. Band calculations[9,10] show that the $5f$ electrons reside in bands that narrow from a width of 2.4 eV for UN to 0.2 eV for UTe as a result of decreasing $f$-$p$ hybridization. A better treatment of Coulomb spin correlations could localize the $f$ electrons and sharpen the one-electron bandwidth even more. The $d$ electrons occupy a band at least 3 eV wide. Since the Fermi energy cuts both these bands, nonintegral numbers of $5f$ and $6d$ electrons are associated with each uranium atom. Experiment supports this picture. Photoemission studies[11,12] show the narrow $5f$ band close to the Fermi level as well as the overlapping $d$ bands. High electronic specific heats[1,13] point to a high density of states at the Fermi level, and the scattering of nearly free conduction electrons into this high density of states gives rise to the metallic resistivity in a two-band model of electron transport.

A number of features of the electronic structure can be identified by examining the systematics of the effective force constants derived from fits to the dispersion relations, as well as the systematics of the elastic constants and bulk modulus. The experimental and calculated[14] bulk moduli decrease with increasing lattice parameter and are largest for UN and smallest for USb in the pnictide series. For ionic insulators like the alkali halides with the rocksalt structure the bulk modulus is roughly inversely proportional to the atomic volume, but the variation with volume for the U$X$ series is much more rapid. The reason appears to be a negative contribution to the bulk modulus from the narrow bands overlapping the conduction band, which grows as the bands sharpen up. Poisson's ratio is small and sometimes negative for the U$X$ compounds with large lattice parameters.

Section II of the paper deals with experimental aspects of the measurements. The results of the analysis are presented and discussed in Sec. III in terms of the electronic structure outlined above.

## II. EXPERIMENTS

The phonon-dispersion relations were determined by inelastic neutron scattering with triple-axis crystal spectrometers operated in the constant-Q mode. In Figs. 1–5 results for the principal crystallographic directions are presented for UC,[4,5] UAs,[6] USb,[6] UN,[7] US,[8] USe, and UTe. All results refer to room-temperature measurements except for UN (Fig. 2), where frequencies at 4.2 K are given. However, in this case a selected number of modes were studied at room temperature, where it was found that frequencies differed by less than 2% from those at 4.2 K. It is also known that the bulk modulus of UN, as calculated from ultrasonic velocity measurements,[15] decreases by less than 1.5% between 4.2 and 300 K. As will be evident, the change in phonon behavior across the U$X$ series is much more dramatic than this and, consequently, comparison of the 4.2-K results for UN with the room-temperature results of the other compounds is justified.

The experiments on USe and UTe were carried out on the C5, N5, and L3 triple-axis crystal spectrometers at the NRU reactor, Chalk River. A summary of the experimental details is given in Table I. Measurements were made with scattered neutron energy $E_1$ fixed at values between 2.5 and 9.0 THz, depending on the desired resolution. Counting times for each phonon varied from a few minutes for acoustic phonons which could be sharply focused to several hours for flat optic-phonon branches. Special care was exercised in the measurement of the acoustic phonons at low wave vectors by reducing $E_1$ to minimize the vertical component of the scattered wave vector $\mathbf{k}_1$. For each measured group a correction for vertical divergence was applied, equal to the difference between the frequency on the model dispersion surface and the peak position of a neutron group computed by folding the model dispersion surface with the experimental resolu-

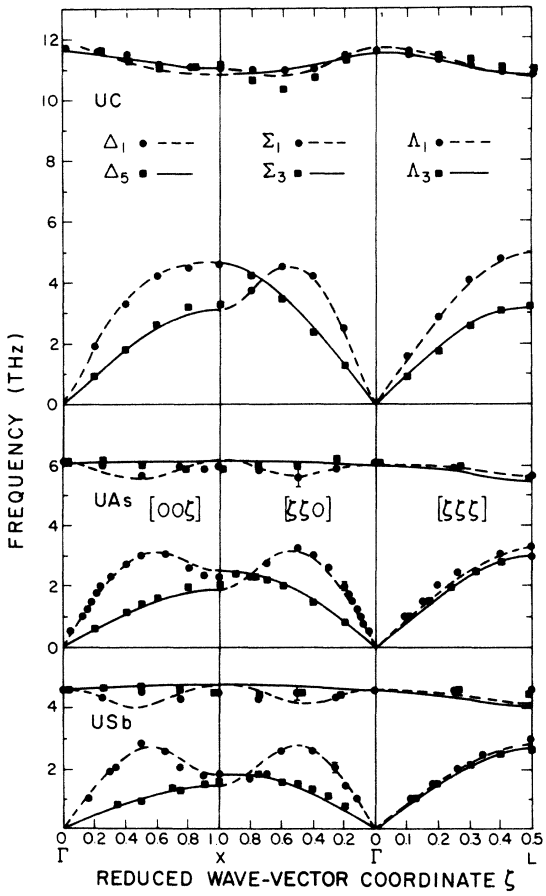


FIG. 1. Frequency versus reduced wave vector, $\zeta$ (units of $2\pi/a$, where $a$ is the lattice parameter), dispersion relation for phonons propagating in the principal directions in UC, UAs, and USb at room temperature. Solid (transverse modes) and dashed (longitudinal modes) curves represent least-squares fits of the rigid-ion model to the experimental data.

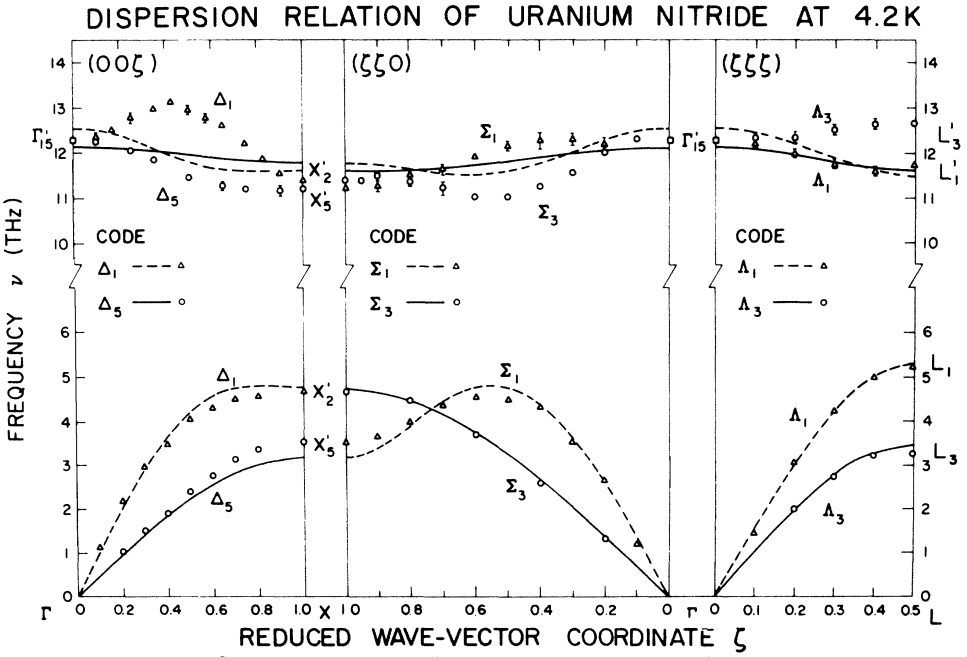


FIG. 2. Phonon-dispersion relations for UN at 4.2 K. Solid (transverse modes) and dashed (longitudinal modes) curves represent least-squares fits of the rigid-ion model to the data.

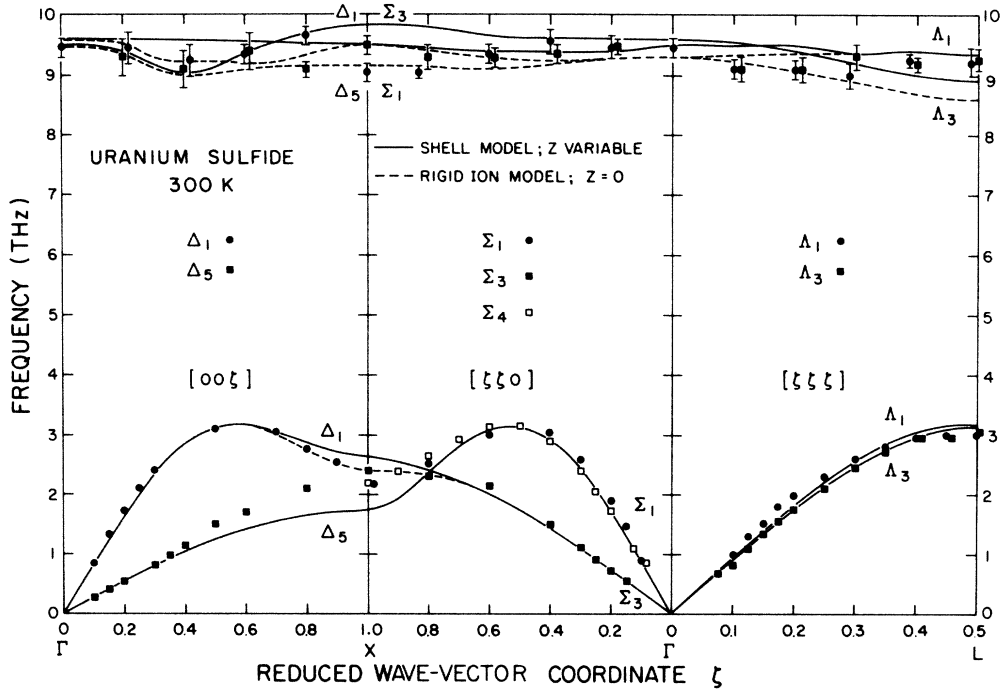


FIG. 3. Phonon-dispersion relation for US at 300 K. Solid and dashed curves represent least-squares fits of shell and rigid-ion models to the experimental data.

tion function, according to the method of Cooper and Nathans.[16] These corrections were less than 5% in each case. In order to find the limiting slopes at small wave vectors the results were plotted as $\nu/\zeta$ versus $\zeta^2$ to obtain the $\zeta=0$ intercept.

From Figs. 3–5 it is seen that the [$\zeta\zeta\zeta$] LA- and TA-phonon branches are fairly close in frequency over the Brillouin zone for the uranium chalcogenides as well as for UAs and USb. It was difficult to measure the [$\zeta\zeta\zeta$] LA frequences with the same accuracy as the other high-symmetry directions. This is because multiply scattered intensity, involving creation of a TA phonon preceded by a Bragg reflection, is observed at positions in reciprocal space where only longitudinal phonons are expected on the basis of the one-phonon cross section. Generally this problem becomes less severe as the Ewald sphere shrinks,

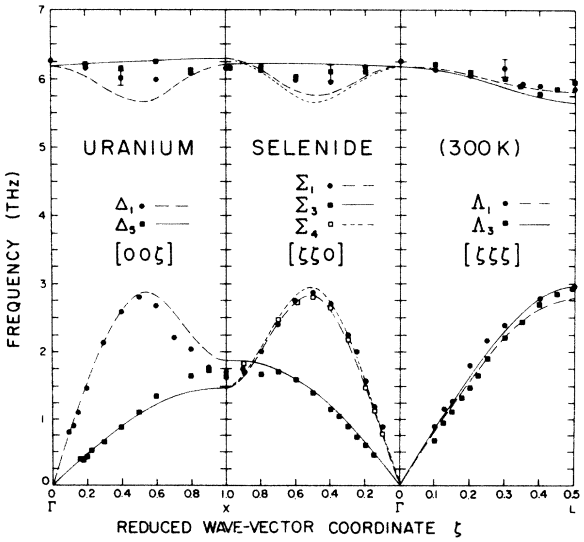


FIG. 4. Phonon-dispersion relation for USe at 300 K. Solid (transverse modes) and dashed (longitudinal modes) curves represent the best fit of the rigid-ion model to the experimental data.

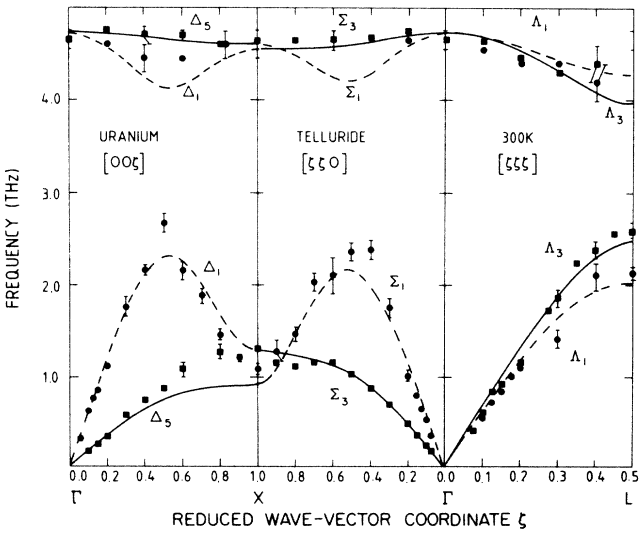


FIG. 5. Phonon-dispersion relation for UTe at 300 K. Solid (transverse modes) and dashed (longitudinal modes) curves represent the best fit of the rigid-ion model to the experimental data.

TABLE I: Experimental details on phonon measurements in uranium chalcogenides: Samples, their volumes $V$, and mosaic spread $\mu_s$; monochromators ($M$) and analyzers ($A$) and their mosaic spread $\mu$; collimation between monochromator and sample ($M$-$S$) and sample and analyzer ($S$-$A$). Pyrolytic graphite monochromators are designated by PG.

| Sample | $V$ (cm$^3$) | $\mu_s$ (deg) | $M$ | $A$ | Collimation (deg) $M$-$S$ | $S$-$A$ |
|---|---|---|---|---|---|---|
| US | 1.5[a] | 0.27[b] | Ge(113) $\mu=0.49°$ | PG(002) $\mu=0.50°$ | 0.7 | 0.9 |
| US | 1.5[a] | 0.27[b] | Si(111) $\mu=0.20°$ | Si(111) $\mu=0.53°$ | 0.8 | 1.0 |
| USe | 0.5 | 0.3 | Si(111) $\mu=0.18°$ | PG(002) $\mu=0.28°$ | 1.16 | 0.67 |
| UTe | 2.0[c] | 1.2 | Be(002) $\mu=0.44°$ | PG(002) $\mu=0.41°$ | 0.7 | 0.8 |
| UTe | 0.3 | 0.2[b] | Si(111) $\mu=0.23$ | PG(002) $\mu=0.28$ | 0.43 | 0.57 |
| | | | Si(111) $\mu=0.23$ | Si(111) $\mu=0.20$ | 0.43 | 0.57 |

[a]Two crystals.
[b]The mosaic spread of the sample was obtained by deconvolution of a measurement of a Bragg peak.
[c]Composite assembly of several crystals.

since there are fewer reciprocal-lattice points in the crystal available for the Bragg scattering event. Identification of the true one-phonon peak requires measurements at several values of $E_1$ since the multiple-scattering intensity depends sensitively on $E_1$, whereas the one-phonon intensity dependence is a slower known function.

There is a further difficulty in the measurement of TA-phonon modes propagating in the $[\zeta\zeta\zeta]$ direction of cubic materials which has emerged several times since the late sixties.[17–19] The two phonon modes with predominantly TA character are only degenerate precisely along the $[\zeta\zeta\zeta]$ symmetry direction, where one mode can be described as polarized along $[1\bar{1}0]$, and is invisible in the $(1\bar{1}0)$ plane, and the second is polarized along $[\bar{1}\,\bar{1}\,2]$ and has maximum intensity. Away from the $[\zeta\zeta\zeta]$ direction, for example, for a slight out-of-plane offset along $[1\bar{1}0]$, the eigenvectors rotate rapidly so that both modes have comparable cross sections; one mode has a frequency which is greater than the on-axis frequency, the other has a lower frequency. Under high-resolution conditions both modes can sometimes be resolved, whereas under low resolution an apparent line broadening can occur.

Because UTe is a fairly well localized magnetic moment system exhibiting sharp spin waves, one might consequently expect a phonon-quadrupolar interaction which would have a strong bearing on the interpretation of its magnetic behavior. Therefore, when an apparent resonance was observed in UTe the effect was examined carefully. Results at 4.2 and 300 K are shown in Fig. 6. It was found, however, that the position of the resonance did not change below the ordering temperature of UTe when the molecular field would certainly shift the crystal-field levels. In addition, the total intensity in the two peaks accurately followed the $(n_\omega+1)$ population factor. A shift

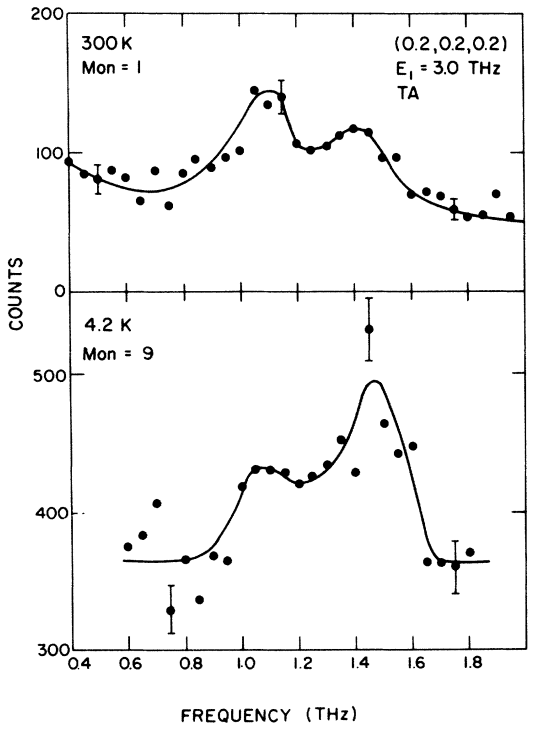


FIG. 6. Spectrum of scattered neutrons for UTe at the reduced wave vector $\zeta=0.2$ $[aQ/2\pi=(-1.8, -1.8, 2.2)]$ showing the two transverse-phonon modes just off the $[\zeta\zeta\zeta]$ high-symmetry axis picked up by the finite-wave-vector resolution of the instrument. The peak positions do not change with the temperature and the integrated intensity follows the $(n_\omega+1)$ population factor.

TABLE II. Lattice constants in angstroms ($a$), radial ($A$) and tangential ($B$) force constants in N m$^{-1}$, and ionic charge, $Z$, derived from fits of the rigid-ion model to the phonon-dispersion relations. Force constants from dispersion relations determined at other institutions are quoted as given in the original literature. Our own fits to their data give force constants that differ insignificantly from the quoted values. Parameters for UP are interpolated.

| | | Force constants (N m$^{-1}$) | | | | | | | | |
|---|---|---|---|---|---|---|---|---|---|---|
| | | U-$X$ | | U-U | | $X$-$X$ | | Ionic charge | |
| Compound | $a$ | $A$ | $B$ | $A'$ | $B'$ | $A''$ | $B''$ | $Z$ | Goodness of fit |
| UC[a] | 4.960 | 44.1 | 2.3 | 38.5 | −0.5 | −0.7 | −0.7 | 0.0 | |
| UN[b] | 4.895 | 51.9±3.1 | 6.3±2.0 | 35.4±2.4 | −1.2±1.2 | −1.6±0.8 | −0.0±0.8 | 0.3±0.1 | 5.2 |
| UP | 5.590 | 63.4 | 5.8 | 5.7 | −0.4 | 1.3 | 0.1 | | |
| UAs[c] | 5.779 | 59.3 | 2.9 | 2.3 | 4.0 | 4.9 | 0.6 | 0.0 | 0.8 |
| USb[c] | 6.205 | 51.3 | 1.8 | 2.7 | 2.1 | 2.2 | 1.9 | 0.0 | 1.1 |
| US[d] | 5.489 | 66.7±2.0 | 7.0±1.4 | −0.8±1.4 | 0.3±0.8 | 3.6±1.4 | −1.4±0.8 | 0.0 | 3.1 |
| USe | 5.744 | 62.3±1.2 | 5.8±0.7 | −3.2±1.0 | −0.5±0.5 | 2.4±1.0 | 1.2±0.5 | 0.0 | 2.9 |
| UTe | 6.155 | 47.5±1.2 | 6.7±0.8 | −6.7±0.8 | −1.2±0.8 | 3.9±1.4 | 0.4±0.8 | 0.0 | 2.2 |

[a]Reference 5.
[b]Reference 7.
[c]Reference 6.
[d]Reference 8.

in the relative intensity of the two peaks could easily be accounted for by the spread in wave vectors generated by the domain structure in the ferromagnetic phase. The correct explanation of the resonance is simply the resolving of the two "TA-like" phonon modes just off the $[\zeta\zeta\zeta]$ symmetry direction. Examination of the eigenvectors confirms this; the lower-mode intensity is stronger than that of the upper mode at $\zeta=0.2$, whereas the reverse is true for $\zeta=0.25$, thus contributing to the apparent effect of a resonance.

## III. ANALYSIS AND DISCUSSION OF THE PHONON-DISPERSION RELATIONS

The dispersion relations for U$X$ compounds were all fitted to the rigid-ion and shell[20] models in order to determine the effective force constants. The rigid-ion model includes radial and tangential short-range force constants between nearest neighbors, U-$X$, and between next-nearest neighbors, U-U and $X$-$X$. The short-range forces are related to the first (tangential) and second (radial) spatial derivatives of the interatomic potential. When the "ionic charge" $Z$ is included there can be seven adjustable parameters to fit to the phonon-dispersion curves. In the shell model each ion is assumed to have an outer spherical shell of electrons coupled to its core. One might associate the outer shell with valence electrons outside a filled shell and hence expect the shell model to provide a better description of the data than the rigid ion. In practice, fits to the shell model are little better than to the rigid-ion model. The rigid-ion model is identical to a short-range axially symmetric force-constant model when $Z=0$. These models, constructed as they were to describe alkali halide crystals, accurately reflect the symmetry of the structure and do identify the principal Fourier components in the spectra but do not have the physics of metallic electrons built into them. Construction of realistic models for U$X$ compounds including, for example, the effects of narrow $5f$ bands and wide $6d$ bands, is beyond the scope of this paper. Nevertheless, the rigid-ion model serves to identify some important trends in the data.

The dispersion relations for UC were fitted accurately[5] by the rigid-ion model, except for the TA $[00\zeta]$ mode near the point $X$ in the Brillouin zone. The force constants are given in Table II. The Coulomb splitting between the LO and TO modes at $\Gamma$ vanishes since UC is metallic and the ion core is well screened. As expected, $Z$ was found to be zero.

By contrast with nonmagnetic UC, a short-range force-constant analysis in UN is unsatisfactory primarily in the region of the optic modes. The calculated optic modes display, at most, an 8% variation in frequency, compared with the observed 14% variation, and the model fails to describe which of the optic modes, TO or LO, lies lowest in frequency in any direction. The model fits the acoustic modes well, except near the $X$ point, as already noted for UC. The fitted ionic charge in the rigid-ion model was again found to be nearly zero, as is to be expected for a metallic compound. Adoption of the shell model did not significantly improve the fit for UN. In going from UC to UN, an increase in the $5f$ density of

states occurs at the Fermi energy, but with little change in lattice parameter. It appears that this gives rise to long-range forces, not described by a short-range model, which particularly affect the optic modes.

Table II shows that the radial U-U force constant ($A'$) is only slightly smaller than the radial U-$X$ force constant ($A$) in UN and UC, indicating that there are strong U-U interactions. The radial $X$-$X$ force constants ($A''$) are more than an order of magnitude weaker. Simple size considerations, from an ionic viewpoint, do not indicate why the U-U force is comparable with, say, the U-N force, and why the N-N force is much smaller than either. The bondlength for U—N is 2.45 Å and for U—U and N—N is 3.46 Å. The sum of the ionic radii[21] of $U^3$ (1.04 Å) and $N^{3-}$ (1.48 Å) is 2.52 Å, indicating that these ions touch, but twice the ionic radius of $U^{3+}$ (2.08 Å) or of $N^{3-}$ (2.96 Å) is much less than 3.46 Å. Therefore, one would expect the U-U forces to be of the same order or less than the N-N forces. Both UN and UC have similar U-U force constants, so that this feature cannot be affected by $5f$ orbitals, but is probably related to the interactions between the more extended $d$ orbitals.

The force constants derived from the rigid-ion fit to the dispersion relations for US (Ref. 8) are also given in Table II. Again, it was found that there is little improvement to the fit when a shell model, rather than a rigid-ion model, is utilized. The results are therefore presented only for the rigid-ion model. The main discrepancies are in the acoustic modes near $X$, in common with UC and UN, and in the more marked frequency dependence of the fitted optic modes compared with experiment. The most unusual feature of US is the near degeneracy of longitudinal and transverse modes in the [$\zeta\zeta\zeta$] and [$\zeta\zeta$0] directions, which leads directly to an anomalously low value of the $C_{12}$ elastic constant (see Table III). This feature is also seen in USe, UAs, USb, and even more strongly in UTe, where the initial slope of the longitudinal-acoustic mode is actually *smaller* than that of the transverse-acoustic mode. Velocity of sound measurements in UTe (Ref. 22) confirm this behavior.

The rigid-ion model fit for USe is shown in Fig. 4 and exhibits the common lack of agreement in the neighborhood of the $X$ point in the Brillouin zone. The derived force constants are given in Table II.

The rigid-ion model is least satisfactory for UTe, as shown in Fig. 5. The model places the LA mode at $X$ above the TA mode, whereas, in fact, the LA mode falls below the TA mode. The maxima in the dispersion relations are not matched by the model and neither is the upward curvature in the $\Sigma_1$ acoustic mode. This suggests a need for further Fourier terms and hence forces that are longer ranged than the nearest- and next-nearest-neighbor forces considered here.

In the chalcogenide series there is a systematic pattern of behavior of the $\Delta_1$ phonons. The ratio of the $X$-point LA frequency to the maximum LA frequency falls from 0.77 (US), to 0.61 (USe), to 0.40 (UTe), suggesting that the $X$-point frequency is being depressed systematically as the lattice parameter falls and the $5f$-band width drops. Within the rigid-ion model the U-U force constant has a major effect on the $X$-point as well as the $L$-point frequency. Figure 7 shows the effect of changing the U-U force constant on model frequencies for UTe while keeping the other force constants the same as determined by the least-squares-fitting procedure. A negative U-U force constant is required to depress the $X$-point frequency, and also to lower the $L$-point LA frequency below the TA frequency. As discussed later, the U-$X$ force constant is practically constant for all the U$X$ compounds.

Phonon frequencies have not yet been measured for UP, but it is possible to interpolate between the force constants of the other U$X$ compounds on the basis of lattice parameter and so to predict the dispersion relation shown in Fig. 8.

The effective radial force constants determined by fitting the rigid-ion model to the experimental dispersion relations vary in a systemic way across the U$X$ series and are plotted in Fig. 9. Apart from the U-$X$ tangential force constant, the other tangential force constants have magnitudes which are only slightly larger than the errors determined in the least-squares-fitting procedure and will not be further discussed. The most obvious feature is that the U-$X$ force constant is dominant and fairly constant across the series. The $X$-$X$ force constant is small throughout the series. The U-U force constant is largest for UC and UN. The most extended electrons on the U site in UC are $6d$ electrons, and we assume that the principal component of the U-U force for UC and probably UN also at this atomic separation is that of $d$ overlap. For UAs and USb the U-U separation is substantially larger, so the $d$-$d$ repulsive contribution is reduced, although—as we see below—there may be a second contribution to the force constant.

The remarkable feature of the U-U force for the chal-

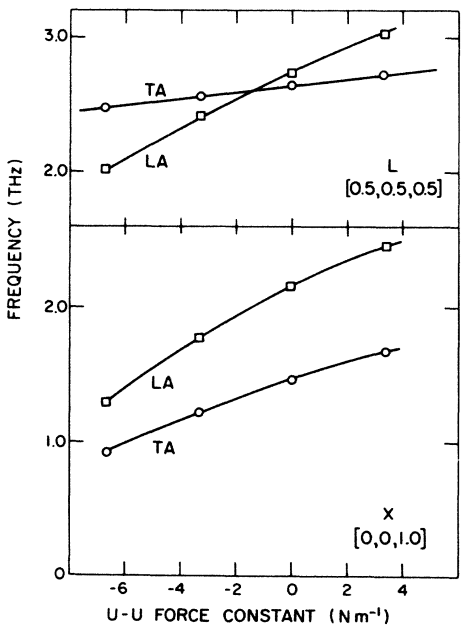


FIG. 7. Model calculations of the frequencies at the $L$ and $X$ points for UTe as a function of the radial U-U force constant, with the other force constants fixed at the values found in the least-squares-fitting procedure.

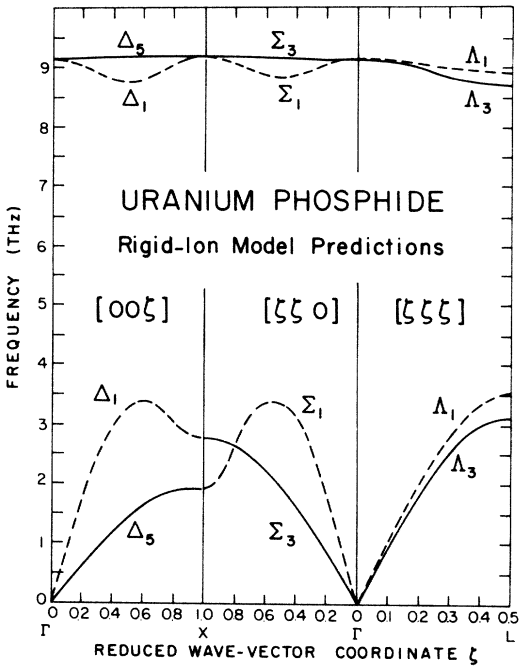


FIG. 8. Phonon-dispersion curves calculated for UP with the rigid-ion model using force constants obtained by interpolation from neighboring compounds to a lattice parameters of 5.590 Å. The phonon-dispersion relation for UP has not yet been measured.

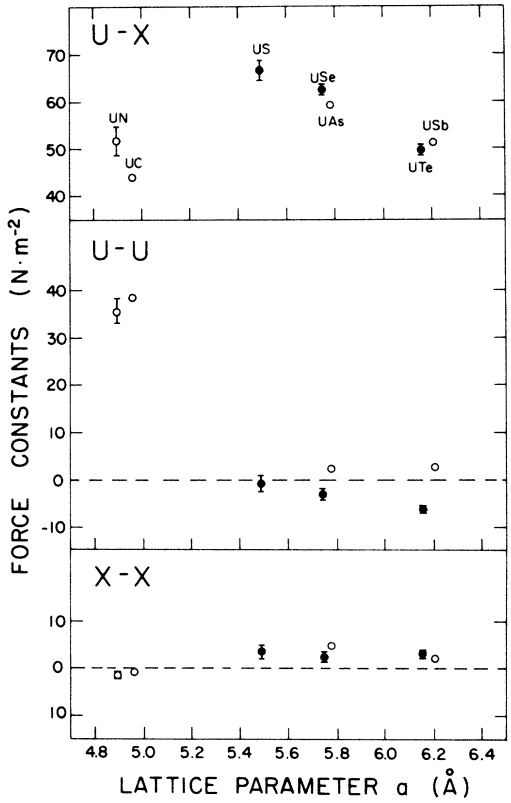


FIG. 9. The U-$X$, U-U, and $X$-$X$ radial force constants determined from the rigid-ion model as a function of lattice parameter. Solid circles represent results for uranium chalcogenides and open circles represent results for uranium pnictides.

cogenides is that it is negative and becomes more so as the lattice parameter increases. As first sight this appears to be an unphysical result, but consideration of the elastic constants, particularly $C_{12}$, indicates why it might be negative. In the mixed-valence materials $Sm_{0.75}Y_{0.25}S$ (Ref. 23) and TmSe (Ref. 24), $C_{12}$ is found to be negative, and it is also small or negative for the U$X$ compounds. In these lanthanide mixed-valence materials, a sharp 4$f$ band overlaps a broader 5$d$ band. Under uniaxial pressure the 5$d$ band widens faster than the 4$f$ band, and there is a transfer from $f$ to $d$ population, a decrease in core screening, and a decrease in ionic size. We believe that there may be a contribution of this kind to the U-U force constant. During a displacement in which the uranium ions move toward each other, some 5$f$ electrons can be transferred to 6$d$ levels, causing a decrease in core screening and a decrease in ionic size. Because it may be favorable for the U-U distance to decrease further, there can be a negative contribution to the U-U force constant. Band-structure calculations[9] show that the 6$d$-band width decreases in the sequence US, USe, UTe. The effect of $f$-$d$ transfer would be expected to be greater for the higher $d$ density of states in a narrower band, and this can provide a qualitative explanation of the decrease in the U-U force constant through the series. On the other hand, the U-$X$ force constant primarily involves $f$-$p$ bonding. Since the $p$ band is already filled, a contribution involving electron transfer will not occur.

It has been noted that the $X$-$X$ force is small for the entire series. This is the opposite of the well-known behavior of the insulating charge-transfer salts, for example, the alkali halides, where the negative ions are larger than the metallic ions and tend to dominate the second neighbor force. The difference undoubtedly distinguishes between a metallic bond involving $s$, $p$, $d$, and $f$ electrons and the quasi-rare-gas configuration of the insulating alkali halides.

The elastic constants $C_{11}$, $C_{12}$, and $C_{44}$, the bulk modulus $B$, and Poisson's ratio $\sigma$ are given in Table III and were obtained by neutron scattering, ultrasonic techniques, or by x-ray measurement of lattice parameters under pressure. For the elastic constants, the precision of the ultrasonic method is often higher than that of the neutron method. It is difficult to determine the frequencies of phonons in the linear part of the dispersion relation at small wave vectors largely because of the errors associated with the vertical divergence correction.

For UN and UC the elastic constants determined from neutron scattering are within one standard deviation of the ultrasonic elastic constants. For UTe the values of $C_{11}$ and $C_{44}$ determined from neutron scattering are within two standard deviations of the ultrasonic values. However, the velocities measured with neutrons for the $[\zeta\zeta 0]_{LA}$, $[\zeta\zeta\zeta]_{TA}$, and $[\zeta\zeta\zeta]_{LA}$ phonons which depend on the $C_{12}$ constant all fall slightly below the velocities calculated from the published ultrasonic constants. Moreover, the three velocities do not lead to a consistent value of $C_{12}$. There is clearly a difference between the behavior in the MHz and THz regions for these modes. A differ-

TABLE III. Elastic constants and bulk modulus ($10^{10}$ N m$^{-2}$) and Poisson's ratio for U$X$ compounds.

| Compound | $C_{11}$ | $C_{12}$ | $C_{44}$ | $B$ | $B$(Theor.)[k] | $\sigma$ |
|---|---|---|---|---|---|---|
| UC[a] | 34.4±4.8 | 10.5±5.6 | 6.1±1.1 | | | |
| UC[b] | 31.49±0.09 | 7.88±0.02 | 6.52±0.02 | 15.75±0.04 | | 0.200±0.002 |
| UN[c] | 39.1±3.6 | 9.0±4.3 | 8.0±1.0 | | | |
| UN[d] | 42.0±0.4 | 9.0±0.5 | 7.9±0.08 | 20.0±0.3 | 21.4 | 0.18±0.02 |
| UN[e] | | | | 20.3±0.6 | | |
| UAs[f] | 25.0±1.0 | 1.0±1.5 | 2.6±0.5 | 9.0±1.3 | 10.6 | 0.04±0.06 |
| USb[f] | 16.0±1.0 | 0.7±1.5 | 2.0±1.0 | 5.8±1.3 | 6.8 | 0.04±0.09 |
| US[g] | 24.5±1.4 | 0.4±0.7 | 2.1±0.1 | 8.4±0.6 | 11.0 | 0.02±0.03 |
| US[h] | 30.17±0.39 | 1.32±0.73 | 1.693±0.019 | 10.7±0.8 | | 0.04±0.02 |
| US[i] | 30.5±1.5 | | 1.72±0.05 | | | |
| US[j] | | | | 9.2±0.9 | | |
| USe | 19.4±1.4 | 0.0±0.7 | 1.6±0.1 | 6.5±0.7 | 9.4 | 0.0±0.3 |
| UTe | 14.9±0.3 | | 1.13±0.04 | | 6.3 | |
| UTe[h] | 14.34±0.36 | −2.0±0.4 | 1.20±0.02 | 3.4±0.6 | | −0.16±0.04 |

[a]Neutrons, Reference 5.
[b]Ultrasonics, Reference 25.
[c]Neutrons, Reference 7.
[d]Ultrasonics, Reference 15.
[e]Compressibility by x-rays, Reference 26.
[f]Neutrons, Reference 6.
[g]Neutrons, Reference 8.
[h]Ultrasonics, Reference 22.
[i]Ultrasonics, Reference 27.
[j]Compressibility by x-rays, Reference 28.
[k]Band theory, Reference 14.

ence between high- and low-frequency velocities can arise from the anharmonic difference between collisionless, or zero, sound and collision-dominated, or first, sound.[29] It is also possible that the phonons interact with the quadrupolar response of the uranium atoms with a characteristic frequency in the THz range.[8] Both effects invalidate the relations between velocities in different directions contained in the theory of elastic waves. These processes cannot be distinguished at present time.

For US the values of $C_{11}$ and $C_{44}$ determined by neutron scattering are about five standard deviations lower (−21%) and higher (+24%), respectively, than the ultrasonic values. These differences between the $C_{11}$ and $C_{44}$ constants measured in the THz neutron region and the MHz ultrasonic region appear to be a real effect, as there are no experimental difficulties such as occur in the determination of $C_{12}$ for these constants. Since the $C_{11}$ elastic constant dominates the velocity where it enters in combination with $C_{44}$ or $C_{12}$, most compressional velocities are reduced at high frequencies. Only the slopes of the transverse modes propagating in the [00$\zeta$] and TA$_1$[$\zeta\zeta$0] directions are enhanced in the high-frequency regime. Consistent with this interpretation the TA[00$\zeta$] phonon branch in US even appears to curve upward well within the Brillouin zone. A possible explanation for this behavior involving phonon-quadrupole interactions was discussed in Ref. 8.

The bulk modulus, $B=(C_{11}+2C_{12})/3$, and Poisson's ratio, $\sigma=C_{12}/(C_{11}+C_{12})$, are plotted in Fig. 10. The bulk moduli[14] calculated from band structure are also shown in Fig. 10 and follow the observed trend correctly. In particular, for compounds with approximately the same lattice parameter (UAs and USe: USb and UTe), the bulk modulus of the pnictide is greater than that of the chalcogenide. However, the band-structure values exceed

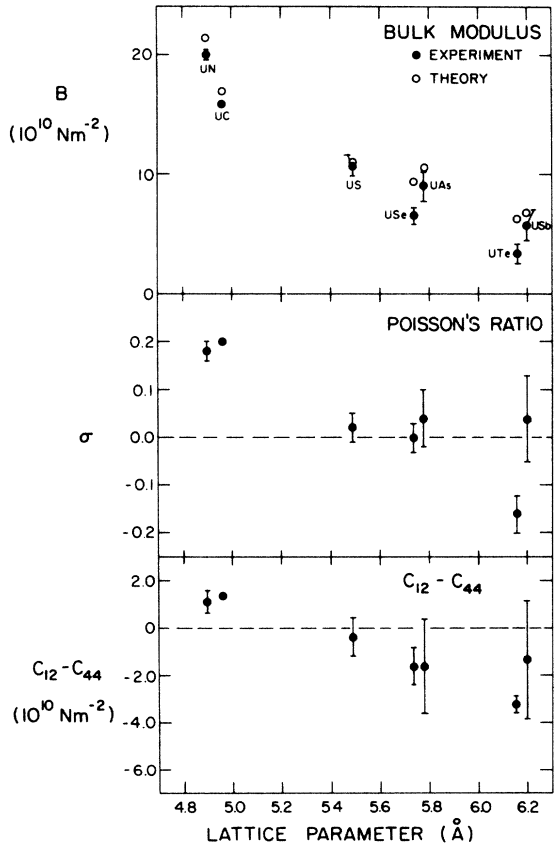


FIG. 10. Bulk modulus, Poisson's ratio, and ($C_{12}-C_{44}$) for U$X$ compounds as a function of lattice parameter. The calculations of bulk moduli from band theory are indicated by open circles.

experiment by 10—20% for the pnictides and by more than 30% for the two chalcogenides with narrowest bands.

The bulk modulus of a series of nonmagnetic compounds is usually inversely proportional to atomic volume. Departures from this situation are observed for both the pnictide and the chalcogenide series. It seems plausible that these departures are caused by a decrease in the electronic contribution to the bulk modulus as the lattice parameter increases. The bulk modulus can be expressed in terms of the atomic force constants in the rigid-ion model. Neglecting the small tangential force constants, we have

$$B=\frac{2}{3a}(A+2A'+2A''+\cdots).$$

A major effect, as we have seen earlier, is the impact of the negative U-U force $A'$; the $f$-$d$ redistribution term tends to destabilize the lattice, while the bonding $A$ term and any $d$-$d$ term in $A'$ tend to stabilize it.

The combination $(C_{12}-C_{44})$ can be crudely identified as the bulk modulus of the conduction electrons.[30] Figure 10 shows that $(C_{12}-C_{44})$ is positive for UN and UC, but negative for all others. It is clear that for large lattice constants this contribution to the bulk modulus is negative and provides a destabilizing influence on the crystal. Because of the imprecision of the tangential force constants, it is not possible to be sure that the U-U force, with its sensitivity to $f$-$d$ fluctuations, does provide the major contribution to $(C_{12}-C_{44})$. However, the common trend in the chalcogenides to smaller values of the U-U force, $\sigma$, and $C_{12}-C_{44}$ makes it likely that this is the case. Finally, we note that $C_{12}$ is anomalously low for U$X$ compounds and is negative for UTe: the low values again indicate the instability of the $5f$-$6d$ system as reflected in the U-U force.

Several models that include electronic effects have been developed for the lattice dynamics of $4f$ mixed-valence systems. One approach[31—33] is to introduce phenomenological "breathing" modes of symmetry $\Gamma_1^+$, dipolar fluctuations $\Gamma_{15}^-$, and quadrupolar fluctuations $\Gamma_{25}^+$ on both metal and ligand sites. In essence, the ligand atoms exert a pressure on the metal ion which causes the valence fluctuation. Bilz *et al.*[33] predicted that the effect of the breathing mode associated with the metal atom is to lower the initial slope of the LA[$\zeta\zeta\zeta$] branch. The effect vanishes at the zone boundary at point $L$ since the lighter ion is stationary. The breathing mode also lowers the frequency of the LO[$\zeta\zeta\zeta$] branch by an amount which is greatest at the $L$ point. Our force-constant results and the lower LA than TA frequency at $(\frac{1}{2}\ \frac{1}{2}\ \frac{1}{2})$ in UTe strongly suggest that the motions of nearest-neighbor uranium ions are primarily responsible for the valence fluctuation rather than the ligand U-$X$ motions.

An alternative model has been proposed by Benneman and Avignon[34] and Entel *et al.*[35] in which the phonons modulate the $f$-$d$ hybridization so that both the $f$-$d$ fluctuation frequency and the hybridization parameter have a linear dependence on the local compression of the lattice. In terms of energy change per unit displacement, the mechanism of Entel *et al.* corresponds to a large electron-phonon interaction.

These models are only superficially relevant for U$X$ compounds because, although they can account for the softening of the LA[$\zeta\zeta\zeta$] branch and for negative values of $C_{12}$, the experimental depression of the LA[$\zeta\zeta\zeta$] branch of the U$X$ compounds is uniform across the zone and does not show a maximum at midzone wave vectors. In addition, the LO[$\zeta\zeta\zeta$] branch of U$X$ compounds, with the exception of UN, is rather flat and only dips slightly in frequency toward the $L$ point of the Brillouin zone, unlike[23] the same branch in $Sm_{0.75}Y_{0.25}S$. We conclude that these classes of phonon models do not contain the physical features required to account for the lattice dynamics of U$X$ compounds. Basically, a successful model has to incorporate redistribution of electrons between next-nearest-neighbor uranium ions, rather than with the $X$ nearest neighbors, since it is the U-U force constant which shows unusual systematic behavior.

## ACKNOWLEDGMENTS

We wish to thank W. J. Stirling and G. H. Lander for providing tables of phonon frequencies for UAs and USb, and G. Dolling for many useful discussions. Expert technical assistance by H. F. Nieman, D. C. Tennant, J. C. Evans, M. M. Potter, A. H. Hewitt, and N. J. S. Grobler is acknowledged. J. A. Jackman is grateful to the Natural Sciences and Engineering Research Council (NSERC) of Canada for financial aid, and P. de V. DuPlessis is grateful to the South African Council of Scientific and Industrial Research and to the Atomic Energy Corporation of South Africa limited for financial assistance.

[1]P. Erdös and J. M. Robinson, *The Physics of the Actinide Compounds* (Plenum, New York, 1983).

[2]*Handbook on the Physics and Chemistry of the Actinides, Parts I and II,* edited by A. J. Freeman and G. H. Lander (North-Holland, Amsterdam, 1984).

[3]W. J. L. Buyers, T. M. Holden, J. A. Jackman, A. F. Murray, P. de V. DuPlessis, and O. Vogt, J. Magn. Magn. Mater. **31-34**, 229 (1983).

[4]H. G. Smith and W. Gläser, in *Phonons: Proceedings of the International Conference, Rennes, France, 1971,* edited by M. A. Nusimovici (Flammarion, Paris, 1971), p. 145.

[5]H. G. Smith, in *Superconductivity in d- and f-Band Metals,* edited by D. H. Douglass (AIP, New York, 1972), p. 321.

[6]W. G. Stirling, G. H. Lander, and O. Vogt, J. Phys. C **16**, 4093 (1983).

[7]G. Dolling, T. M. Holden, E. C. Svensson, W. J. L. Buyers, and G. H. Lander, in *Phonons: Proceedings of the International Conference on Lattice Dynamics, Paris, 5—7 Sept. 1977,* edited

by M. Balkanski (Flammarion, Paris, 1978), p. 81.
[8]P. de V. DuPlessis, T. M. Holden, W. J. L. Buyers, J. A. Jackman, A. F. Murray, and C. F. Van Doorn J. Phys. C **18**, 2809 (1985).
[9]M. S. S. Brooks and D. Glötzel, Physica **102B**, 51 (1980).
[10]M. S. S. Brooks and D. Glötzel, J. Magn. Magn. Mater. **15-18**, 873 (1980).
[11]W. Eib, M. Erbudak, F. Greuter, and B. Reihl, Phys. Lett. **68A**, 391 (1978).
[12]M. Erbudak and F. Meier, Physica **102B**, 134 (1980), and references therein.
[13]H. Rudigier, C. Fierz, H. R. Ott, and O. Vogt, Solid State Commun. **47**, 803 (1983).
[14]M. S. S. Brooks, J. Phys. F **14**, 639 (1984); **14**, 653 (1984).
[15]C. F. van Doorn and P. de V. DuPlessis, J. Magn. Magn. Mater. **5**, 164 (1977).
[16]M. J. Cooper and R. Nathans, Acta. Crystallogr. **23**, 357 (1967).
[17]G. Raunio, L. Almqvist, and R. Stedman, Phys. Rev. **178**, 1496 (1969).
[18]E. R. Cowley and A. K. Pant, Acta. Crystallogr. Sect. A **26**, 439 (1970).
[19]S. A. Werner and R. Pynn, J. Appl. Phys. **42**, 4736 (1971).
[20]A. D. B. Woods, W. Cochran, and B. N. Brockhouse, Phys. Rev. **119**, 980 (1960); R. A. Cowley, W. Cochran, B. N. Brockhouse, and A. D. B. Woods, *ibid.* **131**, 1030 (1963).
[21]G. S. Zhdanov, *Crystal Physics* (Oliver and Boyd, Edinburgh, 1965).
[22]J. Neuenschwander, H. Boppart, J. Schoenes, E. Voit, O. Vogt, and P. Wachter, in *14th Journées des Actinides,* edited by J. Schoenes (Eidgenössiche Technische Hochschule, Zürich, 1984), p. 30.
[23]H. A. Mook and R. M. Nicklow, Phys. Rev. B **20**, 1656 (1979).
[24]H. Boppart, A. Treindl, and P. Wachter, in *Valence Fluctuations in Solids,* edited by L. M. Falicov, W. Hanke, and M. B. Maple (North-Holland, Amsterdam, 1981), p. 103.
[25]J. L. Routbort, J. Nucl. Mater. **40**, 17 (1971).
[26]J. S. Olsen, L. Gerward, and U. Benedict, J. Appl. Crystallogr. **18**, 37 (1985).
[27]P. de V. DuPlessis and D. L. Tillwick, J. Appl. Phys. **50**, 1834 (1979).
[28]J. S. Olsen, S. Steenstrup, L. Gerward, U. Benedict, J. C. Spirlet, and G. D. Andreetti, J. Less-Common. Met. **98**, 291 (1984).
[29]E. C. Svensson and W. J. L. Buyers, Phys. Rev. **165**, 1063 (1968).
[30]J. de Launay, in *Solid State Physics—Advances in Research and Applications,* edited by F. Seitz and D. Turnbull (Academic, New York, 1956) Vol. 2, p. 283.
[31]P. B. Allen, Phys. Rev. B **16**, 5139 (1977).
[32]N. Wakabayashi, Solid State Commun. **23**, 737 (1977).
[33]H. Bilz, G. Güntherodt, W. Kleppman, and W. Kress, Phys. Rev. Lett. **43**, 1998 (1978).
[34]K. H. Benneman and M. Avignon, Solid State Commun. **31**, 645 (1979).
[35]P. Entel, N. Grewe, M. Sietz, and R. Kowalski, Phys. Rev. Lett. **43**, 2002 (1979).